

Adjusted linear quadratic regulator-proportional-derivative control of Quanser's three degrees of freedom helicopter based on flower pollination algorithm under external disturbances

Imam Barket Ghiloubi¹, Latifa Abdou^{1, 2}, Oussama Lahmar¹

¹Identification, Control, Command and Communication Laboratory LI3CUB, Mohamed Khider University, Biskra, Algeria

²Department of Electronics, Faculty of Technology, Mostefa Ben Boulaïd University, Batna, Algeria

Article Info

Article history:

Received Apr 30, 2024

Revised Aug 31, 2024

Accepted Sep 17, 2024

Keywords:

Adjusted linear quadratic regulator
Disturbance
Flower pollination algorithm
Proportional-derivative
Saturation
Three degrees of freedom helicopter

ABSTRACT

External disturbances, saturation of actuator motors, and limits of certain angular movements are commonly encountered in robotic systems, particularly those involving flight, and they present the most common and influential factors affecting the stability and performance of these systems. In this paper, a hybrid controller for a three-degree-of-freedom (3-DoF) helicopter is designed and applied to this flying robot system, taking into account the previously mentioned constraints. The proposed hybrid controller integrates proportional-derivative (PD) control with an adjusted linear quadratic regulator (ALQR) using the flower pollination algorithm (FPA) optimization method. Simulation results of travel (λ), elevation (ε), and pitch (ρ) responses, as well as experimental results of elevation and travel tracking responses under external disturbances using the bench-top Quanser's (3-DoF) helicopter, demonstrate the robustness and good performance of the controlled system using the proposed method. The effectiveness of the proposed method is compared to several methods in the literature.

This is an open access article under the [CC BY-SA](#) license.



Corresponding Author:

Imam Barket Ghiloubi

Identification, Control, Command and Communication Laboratory LI3CUB, Mohamed Khider University
Biskra, Algeria

Email: imam.ghiloubi@univ-biskra.dz

1. INTRODUCTION

The control of unmanned aerial vehicle (UAV), including the 6-degree-of-freedom (DoF) hexarotor, 6-DoF quadrotor, or 3-DoF helicopter, is developing by the increase of their uses in different fields, nevertheless the uncertainty of this flying robot and external disturbances such as the disturbance produced by the wind or by an instantaneous shock with another body as well as the constraint of the value limits of some DoF impose some difficulties on the system mathematical model, which requires an efficient and robust controller which must be tested taking these constraints into consideration.

Quite a few control methods are proposed to ensure 3-DoF helicopter control using linear, non-linear, and artificial intelligence techniques and algorithms. A feedback-linearization is applied to the 3-DoF helicopter to control the trajectory tracking with a real-time implementation under disturbance [1]. Boby *et al.* [2] proposed an adaptive controller for nonlinear systems, applying it to the 3-DoF helicopter system whose adaptation is based on quantitative feedback theory (QFT). An adaptive controller is also proposed in [3], considering an external disturbance and motor fault. By combining type 2 fuzzy logic and adaptive control, a hybrid controller is developed to make the trajectory tracking of the 3-DoF helicopter system [4].

Non-linear controllers are used in literature to control the studied system in this paper, such as the backstepping controller implemented in [5] with a disturbance observer and uncertainty, and the continuous

differentiator controller presented in [6] based on sliding mode control and experimentally validated on the 3-DoF helicopter under external disturbances. Proportional-integral-derivative (PID) controller is designed and self-tuned to ensure the control of a 3-DoF helicopter whose results are experimentally validated on the bench-top of Quanser [7]. The hybrid controller featured in [8] combines a linear quadratic regulator (LQR) optimized using a genetic algorithm and PID controller to stabilize the 3-DoF helicopter after modeling the state space model of the system.

In [9], a model reference adaptive controller is developed for elevation angle control of the 3-DoF helicopter based on a neural network using the Lyapunov function to update the control law. Motion control based on backstepping and fuzzy logic with an active disturbance rejection controller (ADRC) is developed for the control of a 3-DoF helicopter [10]. Logic fuzzy controller is optimized in [11] using a modified particle swarm optimization (PSO) to apply simulation control on the 3-DoF helicopter model. Other works also use the backstepping controller to control the 3-DoF helicopter. Gao and Fang [12] propose an adaptive integral backstepping algorithm to improve the robustness of the controlled system by estimating online uncertainty, and Yu *et al.* [13] present a signal compensation technique and a decentralized backstepping control with experimental validation of obtained results.

Without using angular velocity feedback, Liu *et al.* [14] propose a robust optimal control to make a tracking control of 3-DoF helicopter elevation and pitch angles with an output compensator to minimize the uncertainty of the system. In [15], a robust position control is proposed and applied to the previous system under time varying wind disturbances with an experimental validation on Quanser's helicopter bench-top. To achieve trajectory tracking, a robust controller based on the feedback linearization technique (FLT) is implemented on a 3-DoF helicopter [16]. This controller first utilizes the LQR, followed by the signal compensation technique (SCT). Another controller for the same purpose is proposed in [17] without control design or information about the system, so the results are experimentally validated.

When there is a fault in the helicopter's organs, the system's performance is directly influenced and this can be considered as an internal disturbance. In this context, Wang *et al.* [18] propose a controller in the case where the sensor is faulty based on a fault detection and isolation (FDI) observer which also works as a state estimator to allow the proposed fault tolerance controller to ensure accepted performances. Another fault tolerance controller is proposed in [19]. This time, in the event of an actuator fault, it utilizes a neural network observer to mitigate external disturbances and ensure fault tolerance. Subsequently, the stability is analyzed using the Lyapunov method.

In [20], a free controller model is proposed to control a 3-DoF helicopter in real-time. It is based on linear control as a first step then on compensation developed through an uncertainty and external disturbances estimator. A combination of feedback linearization and fractional order sliding mode is presented in [21] to control the 3-DoF helicopter without requiring measurement or estimation of the disturbance whose simulation results are compared with the integer order sliding mode controller. Three controllers are designed for nonlinear systems: state-dependent Riccati equation (SDRE), model reference adaptive control, and sliding mode control which are applied to the 3-DoF helicopter as a nonlinear system [22].

A 3-DoF helicopter control is ensured using PID based on LQR where gains of PID are approximated from the LQR matrix in [23] and another PID controller is applied experimentally to 3-DoF helicopter Quanser's bench-top in [24] after modeling and simulation of controlled system. In the same context, a model predictive control (MPC)-based LQR controller is applied to the previous bench-top [25]. Using successive linearization, nonlinear model predictive control (NMPC) is developed in [26] to control travel and elevation angles of the studied helicopter system, and simulation results are discussed and compared with linear model predictive control (LMPC). Mehndiratta and Kayacan [27] implemented a nonlinear moving horizon estimation (NMHE) and extended Kalman filter (EKF) with nonlinear model predictive control (NMPC) for trajectory tracking of a laboratory 3-DoF Helicopter Quanser. Choudhary [28] proposes to control the 3-DoF helicopter based on the H_∞ method, where the modeling system is divided into 3 sub-systems, each one is a SISO model which governs an angular movement: elevation, pitch, and travel angles under external disturbance.

In the second section, a comprehensive theoretical overview of the system and its state-space model, developed by Quanser, is presented and explained. In the third section, the method proposed in this study is detailed, beginning with the adjusted linear quadratic regulator (ALQR). Next, the application of the flower pollination algorithm (FPA) to the regulator is explained, followed by the incorporation of the proportional-derivative (PD) controller into the general structure of the proposed method.

The obtained results are presented in the last section, divided into 2 parts: simulation and experimental results, with an application of impulse disturbance to verify the robustness of the proposed control strategy. The results are discussed from the point of view of precision, speed, stability, and robustness. A conclusion at the end of the paper explains and includes a comparison with other works previously carried out.

2. COMPREHENSIVE THEORETICAL BASIS

To study and test the control techniques, it is necessary to have an overview of the 3-DoF helicopter system laboratory robot which is built by “Quanser”. It is mainly composed of two motors to make the angular movements of the helicopter body: elevation ε , pitch ρ , and travel λ with 3 position sensors to provide feedback signals to the controller indicating the response of mentioned angular positions as shown in Figure 1. For making the relationship between the real helicopter and the laboratory 3-DoF Quanser helicopter, Figures 2(a) and 2(b) present a projection of the angular movements of the system around elevation, pitch, and travel axis on a real Boeing helicopter.



Figure 1. Quanser's 3-DoF helicopter [29]

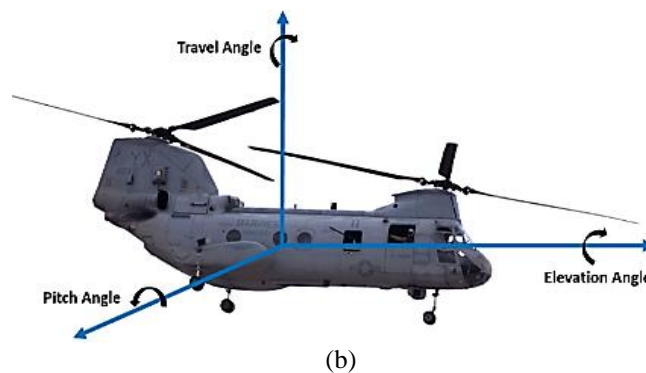
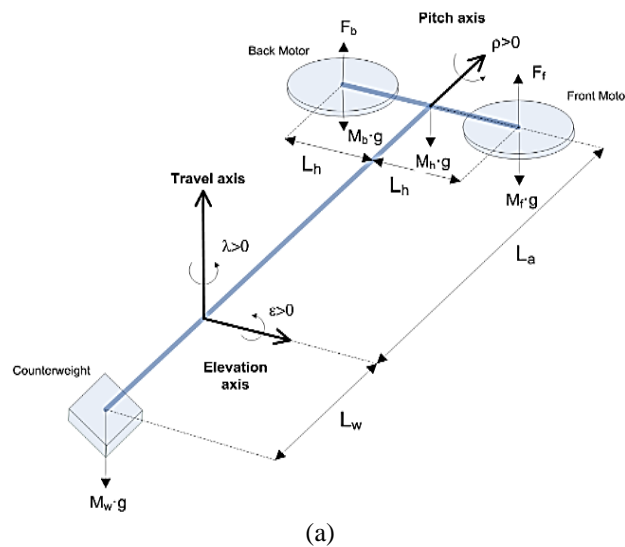


Figure 2. Forces and motion diagram: (a) 3-DoF helicopter's free-body diagram of [29] and (b) free-body diagram translation onto helicopter Boeing CH-47

The 3-DoF helicopter is a system of two inputs: motor input signals and 3 outputs which are elevation ε , pitch ρ , and travel λ angular positions, making it an under-actuated system. The state space model is developed through the linearization of the non-linear model around the operating point by the Quanser constructor [29].

$$\dot{X} = A.X + B.U \quad (1)$$

$$Y = C.X + D.U \quad (2)$$

The state vector, the control vector, and the output vector are presented successively as (3) and (4).

$$X^T = [\varepsilon \quad \rho \quad \lambda \quad \dot{\varepsilon} \quad \dot{\rho} \quad \dot{\lambda}] \quad (3)$$

$$U^T = [U_f \quad U_b] \quad (4)$$

$$Y^T = [\varepsilon \quad \rho \quad \lambda] \quad (5)$$

U_f is the control input signal of the front motor and U_b is the control input signal of the back motor. The final state space model is (6) and (7).

$$\dot{X} = \begin{bmatrix} 0 & 0 & 0 & 0 & 0 & 0 \\ 0 & 0 & 0 & 0 & 0 & 0 \\ 0 & 0 & 0 & 0 & 0 & 0 \\ 0 & 0 & 0 & 0 & 0 & 0 \\ 0 & 0 & 0 & 0 & 0 & 0 \\ 0 & -\frac{(L_w m_w - 2L_a m_f)g}{m_w L_w^2 + 2m_f L_a^2} & 0 & 0 & 0 & 0 \end{bmatrix} . X + \begin{bmatrix} 0 & 0 \\ 0 & 0 \\ 0 & 0 \\ \frac{L_a K_f}{2m_f L_a^2 + m_w L_w^2} & \frac{L_a K_f}{2m_f L_a^2 + m_w L_w^2} \\ -\frac{1}{2} \frac{K_f}{m_f L_h} & -\frac{1}{2} \frac{K_f}{m_f L_h} \\ 0 & 0 \end{bmatrix} . U \quad (6)$$

$$Y = \begin{bmatrix} 1 & 0 & 0 & 0 & 0 & 0 \\ 0 & 1 & 0 & 0 & 0 & 0 \\ 0 & 0 & 1 & 0 & 0 & 0 \end{bmatrix} . X + \begin{bmatrix} 0 & 0 \\ 0 & 0 \\ 0 & 0 \end{bmatrix} . U \quad (7)$$

3. PROPOSED CONTROL METHOD

Figure 3 shows the application of the proposed control strategy on the 3-DoF helicopter. The general diagram of the hybrid technique explains the combination of the adjusted LQR technique using the FPA optimization and PD controller to generate the signals U_f and U_b and apply them to the flying robot as shown in Figure 3.

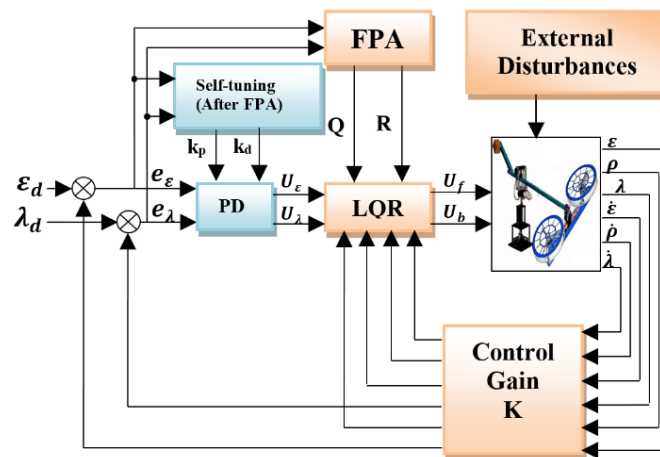


Figure 3. General structure of proposed ALQR-PD control method

3.1. Adjusted linear quadratic regulator

LQR is used to control linear systems or linearized nonlinear systems as in the case of this study, by minimizing an objective function called J index (11) to find the optimal Q and R for calculating final control gain K . This technique is used a lot to control robotics and aerospace systems [25]. The control vector can be calculated using (8),

$$U = -KX \quad (8)$$

where K is calculated using (9).

$$K = R^{-1}B^T P \quad (9)$$

P is a positive definite solution which can be found by solving the Riccati equation in (10).

$$A^T P + PA + Q - PBR^{-1}B^T P = 0 \quad (10)$$

Q is a positive or semi-positive defined symmetric matrix and R is a positive defined symmetric matrix. It is important in this step to find the gains of Q and R matrices used in the previous calculation in such a way that the obtained control gain K is optimal.

For a classic LQR control, the matrices Q and R are chosen to minimize the performance index J .

$$J = \int_0^{+\infty} (X^T Q X + U^T R U) dt \quad (11)$$

The proposed ALQR method is based on the direct minimization of the error between the desired elevation and travel values and the response of each angle instead of minimizing the index J using a metaheuristic optimization technique based on FPA whose objective function is the squared integral error (ISE) which can be written as (12).

$$ISE = \int_0^{+\infty} e_\varepsilon^2(t) + e_\rho^2(t) + e_\lambda^2(t) dt \quad (12)$$

Here, e_ε , e_ρ , and e_λ are the errors between desired and actual values of elevation ε , pitch ρ , and travel λ angles successively [30].

3.2. Application of FPA on LQR

The flower pollination algorithm is one of the metaheuristic optimization methods allowing iteratively to find a desired solution verifying a determined objective function [31]. In this work, FPA is used to find the gains of the matrices Q and R used to calculate the optimal control gain K whose objective function is a function to be minimized presented by the integral squared error ISE between the desired value and the response of the system containing the error of elevation angle and that of travel angle in Figure 4.

Output vector x of the proposed optimization algorithm contains the elements of the best R and Q matrices found after 23 iterations ensuring the appropriate control gain K is considered optimal which makes the system operate with the best error (minimum ISE).

$$Q = \begin{bmatrix} \alpha_1 & 0 & 0 & 0 & 0 & 0 \\ 0 & \alpha_2 & 0 & 0 & 0 & 0 \\ 0 & 0 & \alpha_3 & 0 & 0 & 0 \\ 0 & 0 & 0 & \alpha_4 & 0 & 0 \\ 0 & 0 & 0 & 0 & \alpha_5 & 0 \\ 0 & 0 & 0 & 0 & 0 & \alpha_6 \end{bmatrix} \quad (13)$$

$$R = \begin{bmatrix} \beta & 0 \\ 0 & \beta \end{bmatrix} \quad (14)$$

The objective of FPA is to find the vector x .

$$x = [\alpha_1 \quad \alpha_2 \quad \alpha_3 \quad \alpha_4 \quad \alpha_5 \quad \alpha_6 \quad \beta] \quad (15)$$

Vector x contains the gains of best Q and R matrices used to calculate the optimal control gain K .

$$K = lqr(A, B, Q, R) \quad (16)$$

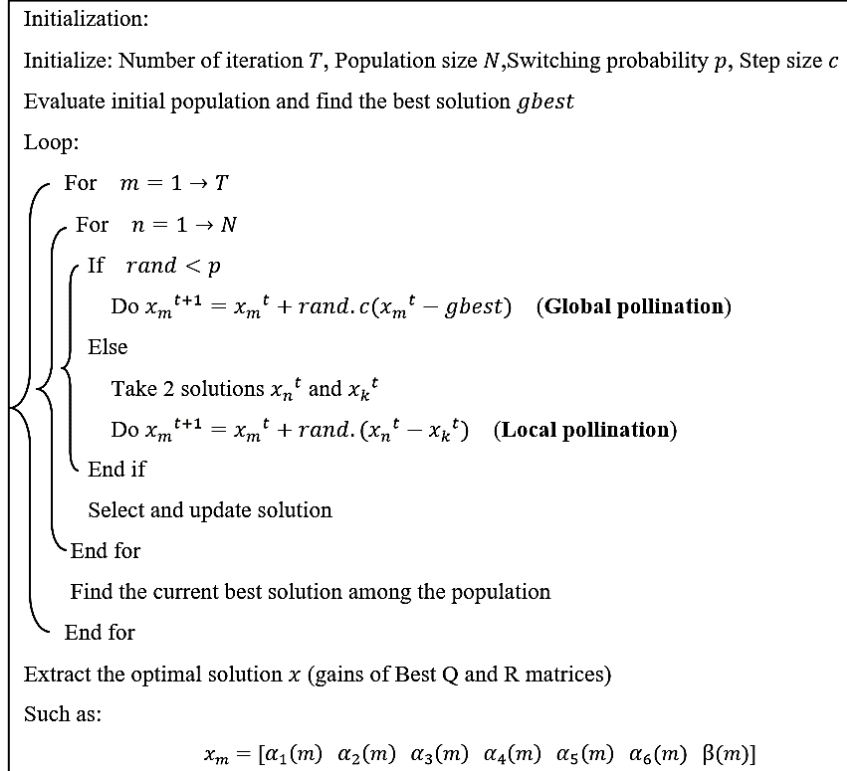


Figure 4. Flower pollination algorithm [30]

3.3. Proportional derivative controller

To ameliorate the performance of the controlled system, a PD controller in Figure 5 is added to the travel loop as well as the elevation loop as shown in Figure 3, where θ_r is the desired angular position (elevation or travel). The PD gains are adjusted manually (self-tuning) until the possible improvement in the response obtained by the ALQR controller occurs in Table 1. MATLAB/Simulink software is used to obtain the results by simulating the controlled system and Quarc software is used to link the Simulink model with the 3-DoF helicopter robot bench-top of Quanser to apply the experimental tests.

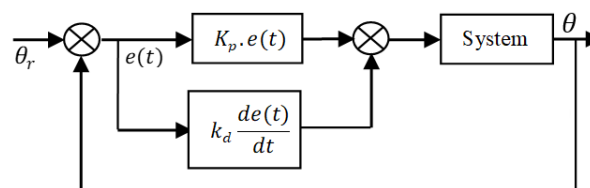


Figure 5. General structure of proposed ALQR-PD control method

Table 1. Self-tuned parameters of PD controller

Angles	Gain K_p	Gain K_d
Elevation ε	8	2.5
Travel λ	2	0.615

4. RESULTS AND DISCUSSION

In this study, the mathematical model parameters mentioned in Table 2 of the manufacturer Quanser are used in the simulation and experimental tests of the system. These parameters include the mass of the front propeller, counterweight, and key distances. They are crucial for ensuring accurate dynamic performance and control of the 3-DoF helicopter system.

Table 2. 3-DoF Quanser's helicopter parameters [29]

Parameter	Symbol	Value
Mass of front propeller assembly (includes motors, shield, propeller and half helicopter body)	M_f	0.713 kg
Mass of the counterweight	M_w	1.87 kg
Propeller force-thrust constant (found experimentally by Quanser)	K_f	0.1188 N/V
Gravitational constant	g	9.81 m/s ²
Distance between travel axis to counterweight	L_w	0.470 m
Distance between travel axis to helicopter body	L_a	0.660 m
Distance between pitch axis to each motor	L_h	0.178 m

4.1. Results of ALQR using FPA

The proposed optimization algorithm parameters are mentioned in Table 3. By applying the proposed metaheuristic technique FPA on the system controller, found Q and R matrices are (17) and (18).

$$Q = \begin{bmatrix} 99.02 & 0 & 0 & 0 & 0 & 0 \\ 0 & 81.05 & 0 & 0 & 0 & 0 \\ 0 & 0 & 100 & 0 & 0 & 0 \\ 0 & 0 & 0 & 0.90 & 0 & 0 \\ 0 & 0 & 0 & 0 & 0.25 & 0 \\ 0 & 0 & 0 & 0 & 0 & 98.47 \end{bmatrix} \quad (17)$$

$$R = \begin{bmatrix} 0.25 & 0 \\ 0 & 0.25 \end{bmatrix} \quad (18)$$

Then, the obtained optimal control gain K is (19).

$$K = \begin{bmatrix} 14.07 & 23.73 & -14.14 & 12.8 & 6.4 & -27.2 \\ 14.07 & -23.73 & 14.14 & 12.8 & -6.4 & 27.2 \end{bmatrix} \quad (19)$$

Obtained control gain K is applied to the general structure of the proposed technique in Figure 3 for the final simulation and experimental applications, where the results obtained are presented in Table 3.

Table 3. FPA parameters

Parameter	Value
Iteration number	$T = 23$
Population	$N = 50$
Search space	$[0 \ 100]$
Output variables	7 variables : From α_1 to α_6 and β
Switch probability	$p = 0.5$
Step size	$c = 0.2$

4.2. Simulation results

The results present steps and tracking responses for each angular position: elevation, travel, and pitch, corresponding to this travel while checking the voltages applied to the helicopter motors and terminated by a table that summarizes the performance of the system controlled by the proposed method.

4.2.1. Elevation angle response

By applying a desired input signal $\varepsilon_d = 7^\circ$, the step response of the system according to the rotation around the elevation axis is presented in Figure 6(a) then a desired sinusoidal input signal $\varepsilon_d = (7.5) \cdot \sin(0.04t)$. The tracking response is presented in Figure 6(b).

According to Figure 6(a), the helicopter's elevation reaches the desired value in a time of less than 1.5 seconds without overshoot and with zero static error, as well as very good tracking of the sinusoidal signal as shown in Figure 6(b) which shows the stability, precision, and speed of the system controlled using the proposed method. Another desired trajectory is applied to the system to check the tracking of the variable steps by the system and the voltages applied to the motors: $\varepsilon_d = [0^\circ \ 15^\circ \ 30^\circ \ 15^\circ \ 0^\circ - 15^\circ - 30^\circ - 15^\circ \ 0^\circ]$ and results are presented in Figure 7.

The system correctly tracks the desired trajectory at the same performance as that of the step response as shown in Figure 7(a) without saturating the motors. Figure 7(b) presents the voltages U_f and U_b

in volts applied by the controller where it is clear that the motors are not saturated and operating at an average voltage do not go out of the interval $[-5 \text{ V } +5 \text{ V}]$, with a pick towards -24 V or $+24 \text{ V}$ at the instants of the step variation which lasts a very small margin of time (10^{-2} second) which is necessary to quickly reach the desired value. To ensure the desired elevation, it is logical that the motors are subjected to the same voltage but the creation of the travel angle requires a movement around the pitch axis achieved by the difference in forces provided by the two motors which interpret the difference between the voltages applied to front and back motor in the first 3 seconds.

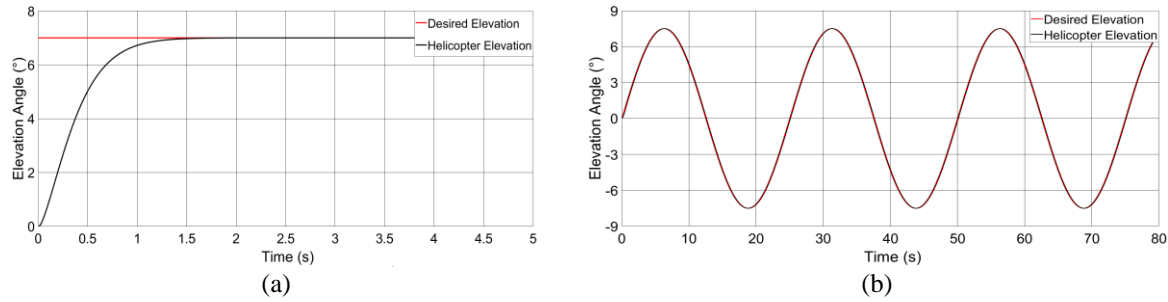


Figure 6. Elevation responses: (a) step response and (b) sinusoidal tracking response

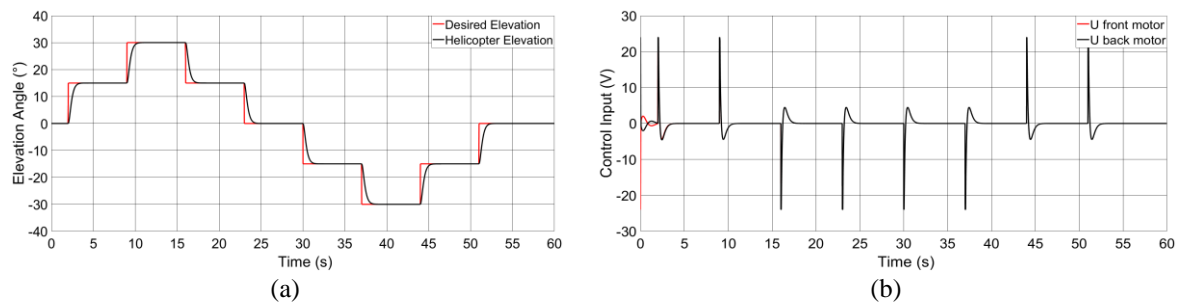


Figure 7. Response and voltages: (a) elevation square tracking response and (b) applied voltages by the controller

4.2.2. Travel and pitch angle response

A set point is applied as the desired value to test the Travel step response of the system: $\lambda_d = 10^\circ$. The helicopter's travel angle reaches the desired travel angle in less than 2.9 seconds and without any overshoot or steady error which shows the accuracy and stability of the proposed method in Figure 8(a) and a very acceptable pitch movement is done by the helicopter to obtain the desired travel in Figure 8(b). Figure 9 shows the step response of the system to a variable desired angular travel position $\lambda_d = [0^\circ \ 15^\circ \ 30^\circ \ 45^\circ \ 30^\circ \ 15^\circ \ 0^\circ - 15^\circ - 30^\circ - 15^\circ \ 0^\circ]$.

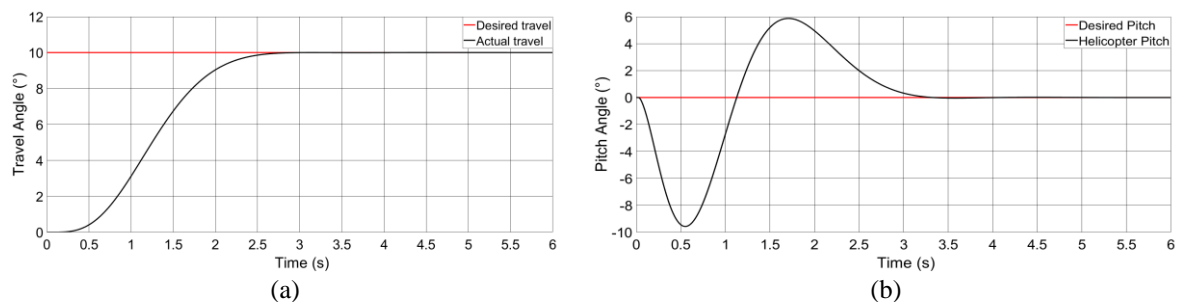


Figure 8. Travel and pitch responses: (a) travel step response and (b) the corresponding pitch response

Figure 9(a) shows that the system follows the desired trajectory with the same performance as the case of the step response, then the proposed method allows the system to function well in different travel angles at a wide interval, from -45° to $+45^\circ$ for example. The pitch angle diverges from 0° towards another value to make an angular movement of the helicopter body around the Travel axis such that the value of the pitch angle does not exceed the limit $[-32^\circ +32^\circ]$ because this limitation is taken into consideration as a constraint in the controlled system in Figure 9(b). Applied voltages in case of travel square tracking are presented in Figure 10.

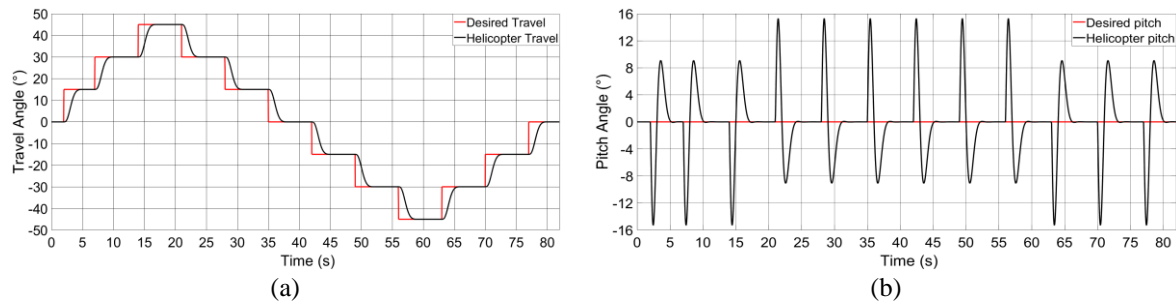


Figure 9. Response and voltages: (a) travel square tracking response and (b) the corresponding pitch response

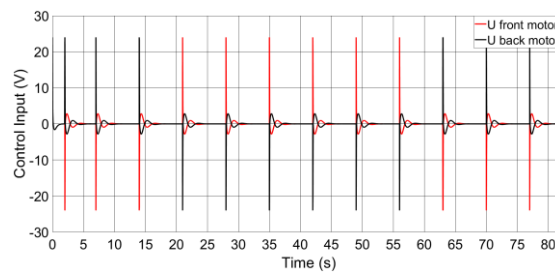


Figure 10. Applied voltages for travel square tracking

With good precision, the suggested controller applies the motor voltages in a balanced manner in Figure 10. The difference in voltages given to the front and back motors at each variation instant of the desired travel step interprets the creation of a pitch angle in Figure 9(b), which in turn generates the desired travel at each instant in Figure 9(a). The success of the suggested solution in real-time application is demonstrated by the fact that the proposed controller does not impose a voltage outside of the interval specified by the manufacturer $[-24\text{ V} + 24\text{ V}]$. The simulation results are summarized in Table 4.

Table 4. Obtained performances using the proposed method

Performances	Settling time (s)	Overshoot (%)	Error (°)
Elevation Angle	< 1.5	0	0
Travel Angle	< 2.9	0	0

These results demonstrate that the proposed method is very well qualified to be validated experimentally because the responses of the system are obtained by taking into consideration the constraints imposed in the system. The limit of the pitch angle is described as

$$\rho = [-32^\circ + 32^\circ]$$

and motor saturation is described as

$$U_{motor} = [-24V + 24V]$$

4.3. Experimental validation results

To validate the simulation results, experimental tests are applied on the bench-top of Quanser's 3-DoF helicopter presented in Figure 11(a) whose parameters are presented in Table 2. Two desired elevations of sinusoidal and variable step form are applied as desired inputs to check the tracking of this angle by the system with manual external disturbances applied to check the fidelity of proposed controller in Figure 11(b) while displaying the voltages applied to each motor (control inputs) in order to confirm the non-saturation of the system's actuators, and the same test is proposed for travel angle with a desired sinusoidal input.



Figure 11. Experimental tests of (a) Quanser's bench-top of 3-DoF helicopter and (b) elevation and travel external disturbance actions (vertical + horizontal)

4.3.1. Elevation response

Figure 12 presents the system response to a step signal input at different amplitudes with the control signals corresponding to this monitoring. A 100-second test is displayed in Figure 12(a), verifying the tracking of the rotation around the elevation axis by the system following the desired trajectory $\varepsilon_d = [-5^\circ \ 0^\circ \ 5^\circ \ 10^\circ \ 5^\circ]$ with the application of a disturbance at the 54th second and a stronger disturbance in the opposite direction at the 62nd second. The system makes a fast return to the desired trajectory in both cases of disturbance with a logical increase in the motor voltages to compensate for the disturbances in the forces applied to the helicopter body in Figure 12(b). Another trajectory is proposed to test the tracking of the elevation angle: $\varepsilon_d = 2 \cdot \sin(0.04t)$ then $\varepsilon_d = (7.5) \cdot \sin(0.04t)$. According to Figure 13, the system correctly follows the sinusoidal trajectory for the two amplitudes: 2° and (7.5°) with a simple error which shows the effectiveness of the proposed method.

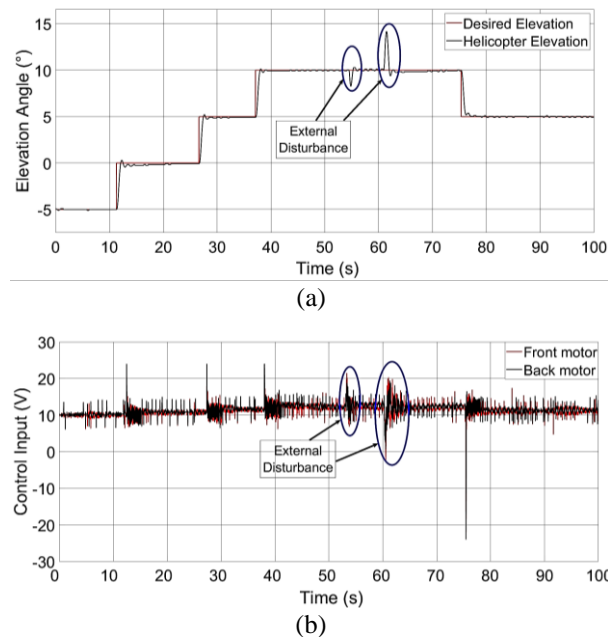


Figure 12. Experimental elevation response: (a) elevation square tracking response under disturbance and (b) applied voltages by the controller

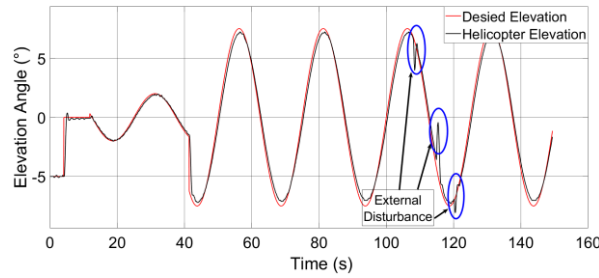


Figure 13. Experimental elevation sinusoidal tracking response under disturbances

4.3.2. Travel response

An experimental test is applied to verify the system response to a desired travel angle λ_d in a sinusoidal form to check the tracking response of the system on the travel axis: $\lambda_d = 45 \cdot \sin(0.03t)$. Depending on the obtained results, the system makes a good tracking of the sinusoidal travel with a simple error as well as a rapid return to the trajectory in the case of an external disturbance like that applied in the 62nd and 103rd seconds of the experimental test in Figure 14(a), where there is a disturbing manual force on the helicopter body applied on the travel axis.

Figure 14(b) explains the balance between the curve of the front motor's voltage (in red) and that of the back motor's voltage (in black), it is remarkable that during the rise of the curve the travel angular movement in Figure 14(a), the back motor is placed at a voltage higher than that applied to the front motor which makes a difference between forces provided by the motors and then creates a positive pitch angle $\rho > 0$ which creates a travel movement λ from -45° to $+45^\circ$ as in the following time interval for example:

$$t \in [8.25 \text{ s } 24.75 \text{ s}]$$

and the opposite is in the following interval:

$$t \in [24.75 \text{ s } 41.25 \text{ s}]$$

where the red curve of the first motor (front) voltage is above that of the second motor (back) voltage, the travel movement is from -45° to $+45^\circ$. It is clear that each of the two voltages has a non-zero average value ($\approx 7 \text{ V}$) and this can be interpreted by maintaining a sufficient value of the elevation angle during the test of this angular travel movement.

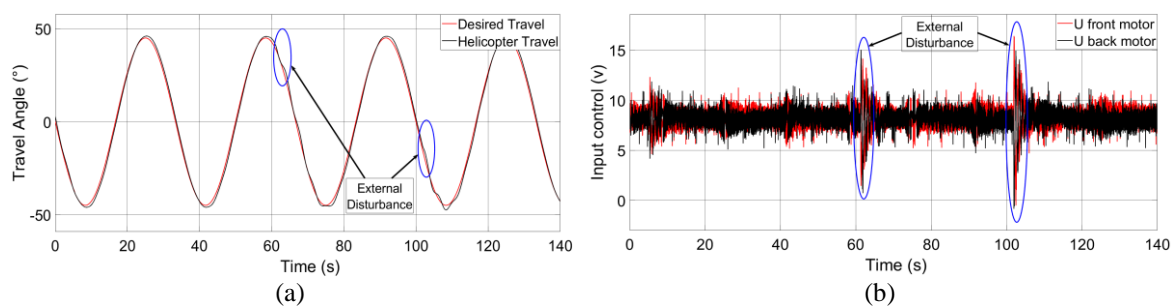


Figure 14. Experimental travel response of (a) travel sinusoidal tracking response under disturbances and (b) applied voltages by the controller

5. CONCLUSION

This paper presents a hybrid control method for 3-DOF helicopters based on the PD controller and ALQR. The ALQR control gain is found through a metaheuristic optimization technique based on FPA passing through 23 calculation iterations, and a PD controller is placed upstream of the travel and elevation angle loop for better performance. Different signals according to each situation are applied to the system as desired values: step, square, and sinusoidal. The simulation results show outstanding responses from the

point of view of stability, precision, speed, and robustness compared to other methods presented previously. Experimental tests are carried out under an impulse disturbance using handle force directly in the case of elevation and travel flight and the results show the effectiveness and robustness of the developed method.




REFERENCES

- [1] N. M. V., M. S. J., and J. Jacob, "Feedback-linearization based robust relatively optimal trajectory tracking controller for 3-DoF helicopter," *Engineering Science and Technology, an International Journal*, vol. 31, Jul. 2022, doi: 10.1016/j.jestch.2021.08.007.
- [2] R. I. Bobby, K. Abdullah, A. Z. Jusoh, N. Parveen, and M. Mahmud, "Adaptive control of nonlinear system based on QFT application to 3-DoF flight control system," *TELKOMNIKA (Telecommunication Computing Electronics and Control)*, vol. 17, no. 5, pp. 2595–2606, 2019, doi: 10.12928/TELKOMNIKA.v17i5.12810.
- [3] K. Yan, M. Chen, Q. Wu, and Y. Wang, "Adaptive flight control for unmanned autonomous helicopter with external disturbance and actuator fault," *The Journal of Engineering*, vol. 2019, no. 22, pp. 8359–8364, Nov. 2019, doi: 10.1049/joe.2019.1080.
- [4] H. Chaoui, S. Yadav, R. S. Ahmadi, and A. E. M. Bouzid, "Adaptive interval type-2 fuzzy logic control of a three degree-of-freedom helicopter," *Robotics*, vol. 9, no. 3, Jul. 2020, doi: 10.3390/robotics9030059.
- [5] R. Mei and Q. Cui, "Backstepping control for a 3DOF model helicopter with input and output constraints," *International Journal of Advanced Robotic Systems*, vol. 14, no. 1, Jan. 2017, doi: 10.1177/1729881416687133.
- [6] H. Castaneda, F. Plestan, A. Chriette, and J. de Leon-Morales, "Continuous differentiator based on adaptive second-order sliding-mode control for a 3-DoF helicopter," *IEEE Transactions on Industrial Electronics*, vol. 63, no. 9, pp. 5786–5793, Sep. 2016, doi: 10.1109/TIE.2016.2569058.
- [7] A. Boubakir, S. Labiod, F. Boudjema, and F. Plestan, "Design and experimentation of a self-tuning PID control applied to the 3DOF helicopter," *Archives of Control Sciences*, vol. 23, no. 3, pp. 311–331, Sep. 2013, doi: 10.2478/acsc-2013-0019.
- [8] I. K. Mohammed and A. I. Abdulla, "Elevation, pitch and travel axis stabilization of 3DOF helicopter with hybrid control system by GA-LQR based PID controller," *International Journal of Electrical and Computer Engineering (IJECE)*, vol. 10, no. 2, pp. 1868–1884, Apr. 2020, doi: 10.11591/ijece.v10i2.pp1868-1884.
- [9] A.-B. Al-Hussein, "Hover control for helicopter using neural network-based model reference adaptive controller," *Iraqi Journal for Electrical and Electronic Engineering*, vol. 13, no. 1, pp. 67–72, 2017, doi: 10.37917/ijece.13.1.9.
- [10] A. N. S. Nam, "Motion control of a three degrees of freedom helicopter," *International Journal of Scientific & Engineering Research*, vol. 11, no. 9, pp. 1120–1127, Sep. 2020, doi: 10.14299/ijser.2020.09.02.
- [11] S. Naderi, M. J. Blondin, and B. Rezaie, "Optimizing an adaptive fuzzy logic controller of a 3-DoF helicopter with a modified PSO algorithm," *International Journal of Dynamics and Control*, vol. 11, no. 4, pp. 1895–1913, 2023, doi: 10.1007/s40435-022-01091-4.
- [12] W.-N. Gao and Z. Fang, "Adaptive integral backstepping control for a 3-DoF helicopter," in *2012 IEEE International Conference on Information and Automation*, Jun. 2012, pp. 190–195, doi: 10.1109/ICInfA.2012.6246806.
- [13] Y. Yu, G. Lu, C. Sun, and H. Liu, "Robust backstepping decentralized tracking control for a 3-DoF helicopter," *Nonlinear Dynamics*, vol. 82, no. 1–2, pp. 947–960, Oct. 2015, doi: 10.1007/s11071-015-2209-8.
- [14] H. Liu, Y. Xi, and Y. Zhong, "Robust optimal attitude control of a laboratory helicopter without angular velocity feedback," *Robotica*, vol. 33, no. 2, pp. 282–294, Feb. 2015, doi: 10.1017/S0263574714000319.
- [15] H. Liu, X. Wang, and Y. Zhong, "Robust position control of a lab helicopter under wind disturbances," *IET Control Theory & Applications*, vol. 8, no. 15, pp. 1555–1565, Oct. 2014, doi: 10.1049/iet-cta.2013.0799.
- [16] H. Liu, Y. Yu, and Y. Zhong, "Robust trajectory tracking control for a laboratory helicopter," *Nonlinear Dynamics*, vol. 77, no. 3, pp. 621–634, Aug. 2014, doi: 10.1007/s11071-014-1324-2.
- [17] C. K. Verginis, C. P. Bechlioulis, A. G. Soldatos, and D. Tsipianitis, "Robust trajectory tracking control for uncertain 3-DoF helicopters with prescribed performance," *IEEE/ASME Transactions on Mechatronics*, vol. 27, no. 5, pp. 3559–3569, Oct. 2022, doi: 10.1109/TMECH.2021.3136046.
- [18] X. Wang, Y. Wang, Z. Zhang, X. Wang, and R. Patton, "Sensor fault tolerant control for a 3-DoF helicopter considering detectability loss," *IEEE Transactions on Circuits and Systems I: Regular Papers*, vol. 70, no. 10, pp. 4112–4125, Oct. 2023, doi: 10.1109/TCSI.2023.3303153.
- [19] M. Chen, P. Shi, and C.-C. Lim, "Adaptive neural fault-tolerant control of a 3-DoF model helicopter system," *IEEE Transactions on Systems, Man, and Cybernetics: Systems*, vol. 46, no. 2, pp. 260–270, Feb. 2016, doi: 10.1109/TSMC.2015.2426140.
- [20] A. Boubakir, S. Labiod, F. Boudjema, and F. Plestan, "Model-free controller with an observer applied in real-time to a 3-DoF helicopter," *Turkish Journal of Electrical Engineering & Computer Sciences*, vol. 22, pp. 1564–1581, 2014, doi: 10.3906/elk-1204-54.
- [21] P. Ahmadi, M. Golestani, S. Nasrollahi, and A. R. Vali, "Combination of two nonlinear techniques applied to a 3-DoF helicopter," *ISRN Aerospace Engineering*, vol. 2014, pp. 1–8, Apr. 2014, doi: 10.1155/2014/436072.
- [22] J. Gu, B. M. Kocagil, A. Ç. Arican, Ü. M. Güzey, S. Özcan, and M. U. Salamci, "Controller designs for nonlinear systems with application to 3 DoF helicopter model," *Gazi University Journal of Science Part A: Engineering and Innovation*, vol. 4, no. 3, pp. 47–66, 2017, [Online]. Available: <http://dergipark.gov.tr/gujsa>.
- [23] S. K. Choudhary, "LQR based PID controller design for 3-DoF helicopter system," *International Journal of Computer, Electrical, Automation, Control and Information Engineering*, vol. 8, no. 8, pp. 1498–1503, 2014.
- [24] H. Desai, "Modelling and control of 3-DoF helicopter," *International Journal for Research in Applied Science and Engineering Technology*, vol. 8, no. 5, pp. 1325–1331, 2020, doi: 10.22214/ijraset.2020.5211.
- [25] O. Lahmar, L. Abdou, and I. B. Ghiloubi, "Quanser's 3-DoF helicopter control using LQR-I and MPC-based LQR controllers," in *2023 International Conference on Control, Automation and Diagnosis (ICCAD)*, May 2023, pp. 1–6, doi: 10.1109/ICCAD57653.2023.10152411.
- [26] Y. Zhai, M. Nounou, H. Nounou, and Y. Al-Hamidi, "Model predictive control of a 3-DoF helicopter system using successive linearization," *International Journal of Engineering, Science and Technology*, vol. 2, no. 10, Mar. 2011, doi: 10.4314/ijest.v2i10.64008.
- [27] M. Mehndiratta and E. Kayacan, "Receding horizon control of a 3 DoF helicopter using online estimation of aerodynamic parameters," in *Proceedings of the Institution of Mechanical Engineers, Part G: Journal of Aerospace Engineering*, Jun. 2018, vol. 232, no. 8, pp. 1442–1453, doi: 10.1177/0954410017703414.
- [28] S. K. Choudhary, " H_∞ loop-shaping controller synthesis for a 3-DoF helicopter system," *Journal of Advanced Research in Dynamical and Control Systems*, vol. 10, no. 15 Special Issue, pp. 490–499, 2018.




- [29] QUANSER, *User manual 3 DoF helicopter experiment*. 2012.
- [30] I. B. Ghiloubi, L. Abdou, and O. Lahmar, "PD-LQR control of 3DOF helicopter using FPA optimization," in *2023 International Conference on Control, Automation and Diagnosis (ICCAD)*, May 2023, pp. 1–6, doi: 10.1109/ICCAD57653.2023.10152309.
- [31] I. B. Ghiloubi, L. Abdou, O. Lahmar, and I. Dahnoun, "3 DoF Quanser's quadrotor control using LQR based on PSO, FPA & ACO with input saturation," in *2023 IEEE 11th International Conference on Systems and Control (ICSC)*, Dec. 2023, pp. 790–795, doi: 10.1109/ICSC58660.2023.10449751.

BIOGRAPHIES OF AUTHORS






Imam Barket Ghiloubi    received a master's degree from the Department of Electrical Engineering/Automatic and Industrial Informatics at the University of Biskra, Algeria, in 2020. He is a Ph.D. student in the Identification, Control, Command and Communication Laboratory LI3cub. He joined the Electrical Engineering Department and Informatics Sciences Department at the same university as an assistant professor. His research interests are focused on the topics of artificial intelligence and autonomous systems control like ground robots, helicopters, drones, multi-agent systems, and optimization techniques applied to the same topics. He can be contacted at imam.ghiloubi@univ-biskra.dz.



Latifa Abdou    received an Engineering degree from the Institute of Electronics at the University of Batna, Algeria, in 1994 and a magister degree at the same institute in 1999. She received her Ph.D. degree in 2009. After graduation, she joined the Electrical Engineering Department at the University of Biskra, then the Technological faculty at the University Mostefa Ben Boulaïd (Batna 2), where she is a professor. She is the head of a research team in the Identification, Control, Command and Communication Laboratory LI3cub. Her research interests are focused on distributed detection systems and the application of heuristic methods in optimisation problems. In addition, she also investigates questions related to automatic systems. She can be contacted at l.abdou@univ-batna2.dz or l.abdou@univ-biskra.dz.



Oussama Lahmar    received a master's degree from the Department of Electrical Engineering/Automatic and Industrial Informatics at the University of Biskra, Algeria, in 2020. He is a Ph.D. student in the Identification, Control, Command and Communication Laboratory LI3cub. His research interests focus on the topics of robotic systems, linear and nonlinear control of autonomous systems, and machine and deep learning. He can be contacted at oussama.lahmar@univ-biskra.dz.